Increased sulfation of bile acids in mice and human subjects with sodium taurocholate cotransporting polypeptide deficiency

Received for publication, December 22, 2018, and in revised form, May 29, 2019 Published, Papers in Press, June 14, 2019, DOI 10.1074/jbc.RA118.007179

Fengfeng Mao,[a,b1] Teng Liu,[c,d,e1] Xinfeng Hou,[b,f1] Hanqing Zhao,[b] Wenhui He,[b] Cong Li,[b,f] Zhiyi Jing,[b] Jianhua Sui,[a,b,g] Fengchao Wang,[b,g] Xiaohui Liu,[h] Jun Han,[i,j] Christoph H. Borchers,[i,j,k,l,m] Jian-She Wang,[c,d2] and Wenhui Li[b,g3]

From the [a]School of Life Sciences, Beijing Normal University, Beijing 100875, China, the [b]National Institute of Biological Sciences, Beijing 102206, China, the [c]Center for Pediatric Liver Diseases, Children's Hospital of Fudan University, Shanghai 201102, China, the [d]Department of Pediatrics, Shanghai Medical College of Fudan University, Shanghai 200333, China, the [e]Department of Pediatrics, Jinshan Hospital of Fudan University, Shanghai 201512, China, the [f]School of Life Sciences, Peking University, Beijing 100091, China, the [g]Tsinghua Institute of Multidisciplinary Biomedical Research and the [h]School of Life Sciences, Tsinghua University, Beijing 100091, China, the [i]UVic-Genome BC Proteomics Centre, University of Victoria, Victoria, British Columbia V8Z 5N3, Canada, the [j]Division of Medical Sciences and [k]Department of Biochemistry and Microbiology, University of Victoria, Victoria, British Columbia V8P 5C2, Canada, and the [l]Gerald Bronfman Department of Oncology and the [m]Proteomics Centre, Segal Cancer Centre, Lady Davis Institute, Jewish General Hospital, McGill University, Montreal, Quebec H4A 3T2, Canada

Edited by Dennis R. Voelker

Sodium taurocholate cotransporting polypeptide (NTCP, encoded by *Slc10a1*/*SLC10A1*) deficiency can result in hypercholanemia but no obvious symptoms in both mice and humans. However, the consequence of and response to long-term hypercholanemia caused by NTCP deficiency remain largely unexplored. Here, we analyzed lifelong dynamics of serum total bile acid (TBA) levels in *Slc10a1*$^{-/-}$ mice, and we also assessed changes of TBA levels in 33 young individuals with *SLC10A1* loss-of-function variant p.Ser267Phe. We found that overall serum TBA levels tended to decrease gradually with age in both *Slc10a1*$^{-/-}$ mice and p.Ser267Phe individuals. Liver mRNA profiling revealed notable transcription alterations in hypercholanemic *Slc10a1*$^{-/-}$ mice, including inhibition of bile acid (BA) synthesis, enhancement of BA detoxification, and altered BA transport. Members of the sulfotransferase (SULT) family showed the most dramatic increases in livers of hypercholanemic *Slc10a1*$^{-/-}$ mice, and one of their BA sulfates, taurolithocholic acid 3-sulfate, significantly increased. Importantly, consistent with the mouse studies, comprehensive profiling of 58 BA species in sera of p.Ser267Phe individuals revealed a markedly increased level of BA sulfates. Together, our findings indicate that the enhanced BA sulfation is a major mechanism for BA detoxification and elimination in both mice and humans with *Slc10a1*/*SLC10A1* deficiency.

Sodium taurocholate cotransporting polypeptide (NTCP,[4] SLC10A1) is localized at the basolateral membrane of hepatocytes and mediates uptake of conjugated bile acids (BAs) (1, 2). It was also identified as an entry receptor for hepatitis B virus and hepatitis D virus (3). *NTCP*/*Ntcp* deficiency has been reported in humans as well as *Ntcp* knockout mice (4–8). In humans, reported pediatric cases with *NTCP* mutation demonstrated more severe hypercholanemia compared with that in adults (4–7), whereas both normocholanemia and hypercholanemia were observed in *Slc10a1*$^{-/-}$ mice at 2 months of age (8). *Slc10a1*$^{-/-}$ mice with hypercholanemia presented with increased renal BA excretion, altered expressions of organic anion transporting polypeptide, and reduction of hepatic BA synthesis (8, 9). However, the long-term consequence of *Slc10a1/SLC10A1* deficiency is unknown.

This work was supported by National Natural Science Foundation of China Grants 81525018 (to W. L.) and 81570468 and 81741056 (to J.-S. W.); Science and Technology Major Project of Beijing Grant D171100003117003 (to W. L.); China Scholarship Council Grant 201606100226 (to T. L.); the Science and Technology Bureau of Beijing Municipal Government (to W. L. and J. S.); the Metabolomics Innovation Centre (TMIC) through the Genome Innovations Network (GIN) from Genome Canada, Genome BC, and Genome Alberta for operations (205MET and 7203) and technology development (215MET and MC3T) (to J. H. and C. H. B.); the Leading Edge Endowment Fund (University of Victoria) and the Segal McGill Chair in Molecular Oncology at McGill University (Montreal, Canada) (to C. H. B.); and the Warren Y. Soper Charitable Trust and the Alvin Segal Family Foundation to the Jewish General Hospital (Montreal, Canada) (to C. H. B.). The authors declare that they have no conflicts of interest with the contents of this article.

This article contains Tables S1 and S2 and Figs. S1–S8.

[1] These authors contributed equally to this work.

[2] To whom correspondence may be addressed: 399 Wanyuan Rd., Shanghai 201102, China. Tel.: 86-21-64931171; E-mail: jshwang@shmu.edu.cn.

[3] To whom correspondence may be addressed: 7 Science Park Rd., ZGC Life Science Park, Beijing 102206, China. Tel.: 86-10-80720039; Fax: 86-10-80726689; E-mail: liwenhui@nibs.ac.cn.

[4] The abbreviations used are: NTCP, sodium taurocholate cotransporting polypeptide; TBA, total bile acids; αMCA, α-muricholic acid; βMCA, β-muricholic acid; ωMCA, ω-muricholic acid; TαMCA, tauro-α-muricholic acid; TβMCA, tauro-β muricholic acid; CA, cholic acid; CDCA, chenodeoxycholic acid; DCA, deoxycholic acid; LCA, lithocholic acid; UDCA, ursodeoxycholic acid; TCA, taurocholic acid; TCDCA, taurochenodeoxycholic acid; TDCA, taurodeoxycholic acid; TLCA, taurolithocholic acid; TUDCA, tauroursodeoxycholic acid; GCA, glycocholic acid; GCDCA, glycochenodeoxycholic acid; GUDCA, glycoursodeoxycholic acid; TLCA-3-sulfate, taurolithocholic acid 3-sulfate; UPLC/MRM-MS, ultra-high performance liquid chromatography/multiple-reaction monitoring–mass spectrometry; UPLC-MS/MS, ultra-performance liquid chromatography-tandem mass spectrometer; TALEN, transcription activator-like effector nuclease.

BAs are cytotoxic when their concentrations reach to abnormally high levels. High-concentration BA can damage cell membranes, increase reactive oxygen species, and induce both apoptosis and necrosis (1, 10). However, no severe abnormality of liver function has been observed in hypercholanemic subjects with *NTCP* mutations reported to date. Similarly, no inflammation or hepatocellular damage was detected in *Slc10a1*$^{-/-}$ mice with hypercholanemia (8). The observations suggest that in both humans and mice with *SLC10A1*/*Slc10a1* deficiency, there are mechanism(s) for detoxification of overload BAs.

Here we combined biochemical assays with RNA profiling studies to investigate the long-term consequence of and the hepatocyte response to the high level BAs in *Slc10a1*$^{-/-}$ mice. We also utilized high-end ultrahigh-performance LC/multiple-reaction monitoring-MS (UPLC/MRM-MS) analysis to profile BAs in individuals whom we identified to harbor the p.Ser267Phe variant in NTCP.[5] Our study reveal that enhanced BA sulfation is a major mechanism for BA detoxification and elimination in both mice and humans with *Slc10a1*/*SLC10A1* deficiency.

Results

Body weight catch-up and serum TBA level reductions in *Slc10a1*$^{-/-}$ mice

The establishment of *Slc10a1*$^{-/-}$ mice was described under "Experimental procedures" (Fig. S1). *Slc10a1* deficiency resulted in dramatic elevation of serum TBA levels in both male and female mice at 8 weeks, and the body weights were inversely correlated with total serum BA levels (8). Here, we confirmed that most *Slc10a1*$^{-/-}$ mice had reduced body weights compared with that of WT littermates starting from post-weaning (day 21; 8 of 11 mice); however, surprisingly, we noted that the body weight of *Slc10a1*$^{-/-}$ mice could catch up with that of WT as age increased (Fig. 1, *A* and *B*). Interestingly, *Slc10a1*$^{-/-}$ mice exhibited various serum TBA levels, from normal (0–20 μM) to extremely high levels (~2 mM) at early ages, and the overall serum TBA levels tended to decrease with age in *Slc10a1*$^{-/-}$ mice (Fig. 1*C*). Nonetheless, some *Slc10a1*$^{-/-}$ mice had TBA levels >100 μM in serum throughout their lifespans (2 of 15 males and 5 of 39 females); however, importantly, the survival of *Slc10a1*$^{-/-}$ mice was not affected under this hypercholanemia by 20 months of age, the end point of the present study (Fig. 1*C*). Profiling of BAs showed that most of the conjugated BAs significantly increased in both male and female mice at 4 weeks (Fig. 2, *A* and *C*). However, at 20 months, male *Slc10a1*$^{-/-}$ mice showed a BA profiling similar to that of WT mice, and some female *Slc10a1*$^{-/-}$ mice still had significant increases in some conjugated BA species, such as TCA, TUDCA, and TCDCA (Fig. 2, *B* and *D*).

TBA levels in individuals with homozygous mutation of p.Ser267Phe in SLC10A1

We recently identified 33 individuals with hypercholanemia who have homozygous mutation of p.Ser267Phe in *SLC10A1*.[5] We retrospectively examined the historical data of serum TBA levels of those individuals who had a TBA test before 1 year old to see if their TBA level also declined over time like what we observed in *Slc10a1*$^{-/-}$ mice. Indeed, TBA levels collected before the age of 100 days were significantly higher than that of following days for those individuals during our follow-ups (Fig. S2*A*). Specifically, 6 of 23 males and 4 of 10 females showed a clear decline of serum TBA levels compared with their early examinations; nine infants exhibited with a fluctuation of TBA levels during the follow-up examinations (Fig. 3 and Fig. S2*B*).

Liver mRNA profiling in *Slc10a1*$^{-/-}$ mice

To decipher the biochemical basis for the declining of TBA levels in the late age of *Slc10a1*$^{-/-}$ mice, we performed a serial liver RNA-Seq analysis of mRNA expression with male mice at 4 weeks, 8 weeks, and 20 months of age, respectively (Fig. S3*A*). At 4 weeks, WT and *Slc10a1*$^{-/-}$ mice exhibited clearly different patterns in terms of transcriptome similarity and were well-separated (Fig. S3, *A* and *B*). However, the difference was indistinguishable at 20 months (Fig. S3*A*). KEGG pathway enrichment analysis showed that the most altered pathways included steroid hormone biosynthesis, chemical carcinogenesis, retinol metabolism, and metabolism of xenobiotics by cytochrome P450 (Fig. 4).

Hepatic gene signature of hypercholanemia in *Slc10a1*$^{-/-}$ mice

We further conducted quantification analysis of the RNA-Seq data, focusing on transcriptional alterations in pathways of BA synthesis, transport, and metabolism. For BA synthesis, *Slc10a1*$^{-/-}$ mice with hypercholanemia exhibited strong reductions relative to WT mice in genes involved in classical BA synthesis (*e.g. Cyp7a1*) and alternative BA synthesis (*e.g. Cyp7b1*) at 8 weeks (Fig. 5*A*); there was a slight decrease of the expression of *Cyp8b1*, which encodes sterol 12α-hydroxylase, an enzyme that directs BA precursors toward hydrophobic BAs at 8 weeks (Fig. 5*A*). As for BA transport, *Slc10a1*$^{-/-}$ mice with hypercholanemia exhibited significantly increased expression of genes encoding transporters that pump BAs into systemic circulation, such as *Abcc3* and *Abcc4*, indicating the enhanced clearance of BAs at 8 weeks (Fig. 5*B*). *Abcb11* and *Abcc2*, which encode transporters responsible for BA efflux into bile, showed no significant differences (Fig. 5*C*). On the other hand, consistent with a previous study (9), genes involved in BA uptake into hepatocytes, *Slco1b2* decreased whereas *Slco1a4* increased, reflecting the maintenance of BA circulation even at high levels of BAs with *Slc10a1* deficiency at 8 weeks (Fig. 5*D*). Meanwhile, genes encoding phase I (*Cyps*) and phase II enzymes (*Sults* and *Ugts*) were induced in *Slc10a1*$^{-/-}$ mice with hypercholanemia at 4 weeks and 8 weeks (Fig. S4, *A*–*C*), consistent with a compensatory mechanism to decrease the overall BA load and to enhance the detoxification reactions in mice. In line with previous findings of BA hydroxylation as a pathway to detoxify overload BAs (11), the mRNA expression level of *Cyp2b10* showed significant increase at 8 weeks (Fig. S5, *A* and *B*), and at the protein level, CYP2B10 significantly

[5] Y. Yan, unpublished data.

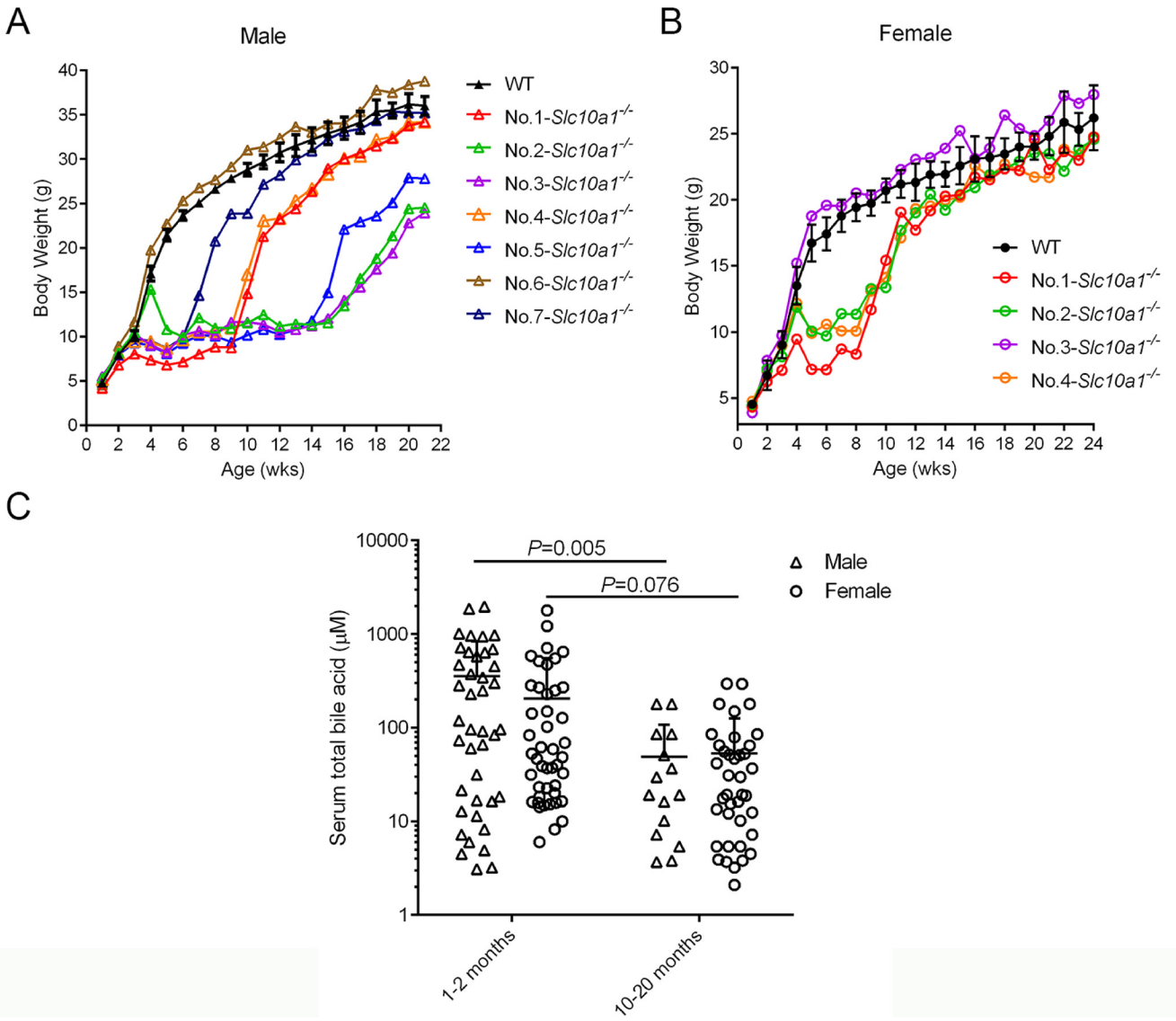

Figure 1. Body weight catch-up and serum TBA level reductions in *Slc10a1*$^{-/-}$ mice. *A* and *B*, individual body weight changes of male (*A*, *No.1–7*) and female *Slc10a1*$^{-/-}$ mice (*B*, *No.1–4*) during a 22-week and 24-week follow-up period, respectively. Body weight in the WT group is shown as mean ± S.D. (*error bars*) of a total of eight mice. *C*, serum TBA levels at 1–2 months and 10–20 months in male and female *Slc10a1*$^{-/-}$ mice, respectively. Data are given on a log-10 scale, and mean ± S.D. values are depicted in the figures (15–45 mice/group). Each *symbol* represents an individual mouse (two-way ANOVA followed by a Bonferroni post hoc test).

increased in half of *Slc10a1*$^{-/-}$ mice (5 of 10 males; Fig. S5*D*); whereas *Sult2a8*, the newly identified hepatic BA sulfotransferase with high activity toward 7α-hydroxylated BAs in mice was significantly decreased in the hypercholanemia mice with *Slc10a1* deficiency at 4 and 8 weeks (12) (Fig. S5*C*).

Regardless of all of these transcription alterations, strikingly, the top five ranked up-regulated genes in male *Slc10a1*$^{-/-}$ mice all belonged to the sulfotransferase (*Sult*) gene family, including *Sult2a1*, *Sult2a2*, *Sult1e1*, *Sult2a6*, and *Sult2a4* (Table 1). Among them, the most up-regulated gene was *Sult2a1*, and its expression was increased more than 1000-fold in *Slc10a1*$^{-/-}$ mice (Table 1). Nuclear receptors have been implicated in orchestrating the various steps involved in BA detoxification, conjugation, and elimination (13, 14). We found that expressions of farnesoid X receptor (*Fxr*), constitutive androstane receptor (*Car*), retinoid X receptor (*Rxra*), and pregnane X receptor (*Pxr*) were increased to different degrees, indicating their potential involvement in regulating of phase I and II detoxification in NTCP-deficient mice (Fig. S6).

Increased taurine-conjugated lithocholic acid-3-sulfate in Slc10a1$^{-/-}$ *mice*

We verified the RNA-Seq results for *Sult2a1* expression using quantitative PCR (qPCR) analysis and Western blotting. Again, qPCR confirmed a more than 1000-fold increase of the *Sult2a1* gene in male *Slc10a1*$^{-/-}$ mice, and at the protein level, *Slc10a1*$^{-/-}$ mice with no CYP2B10 expression showed dramatically increased SULT2A1 (Fig. 6, *A* and *B*). Although *Sult2a1* is one of the most markedly female-predominant *Sult* in mouse liver, the expression of *Sult2a1* also further increased in female *Slc10a1*$^{-/-}$ mice compared with that of WT mice (Fig. S7*A*). SULT2A1 is responsible for the sulfation of BAs, a biochemical process known to reduce BA toxicity and promote the elimination of BAs in humans (13, 15). SULT2A1 plays a significant and

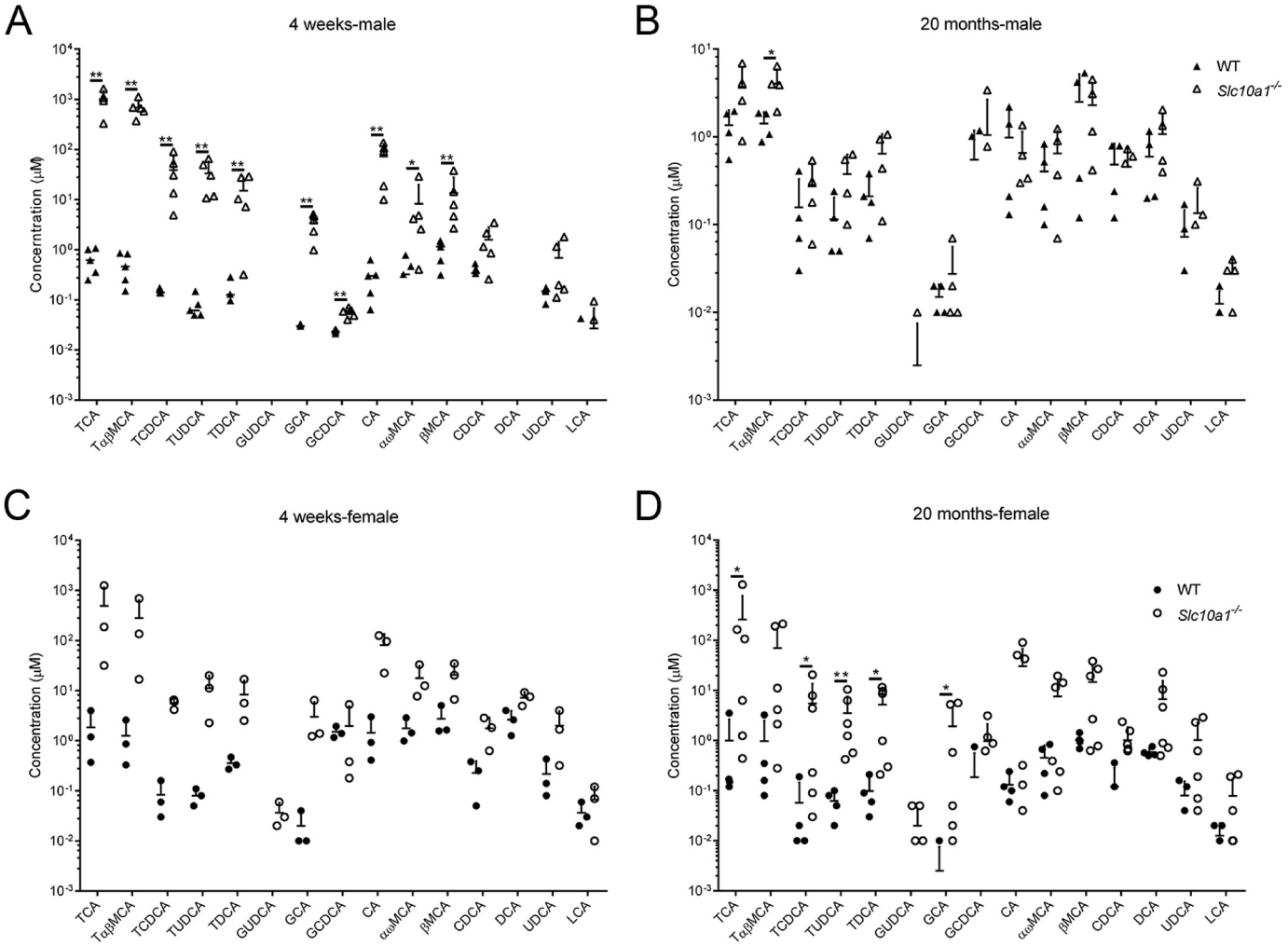

Figure 2. Serum bile acid profiling of the *Slc10a1*$^{-/-}$ mice. Profiling of serum bile acids in male (*A* and *B*) and female (*C* and *D*) WT and *Slc10a1*$^{-/-}$ mice at 4 weeks and 20 months, respectively. BA species were quantified using UPLC-MS/MS. Data are given as mean ± S.D. (*error bars*) on a log-10 scale for 3–6 mice in each group. A mouse with BA species under the detection limit was not presented. *, $p < 0.05$; **, $p < 0.01$, two-tailed Mann–Whitney *U* test.

unique role in 3-hydroxyl group sulfation, particularly in sulfation of LCA and TLCA (16). To verify whether BA sulfation activity was activated under hypercholanemia in *Slc10a1*$^{-/-}$ mice, we measured serum LCA-3-sulfate and TLCA-3-sulfate levels in *Slc10a1*$^{-/-}$ and WT mice with UPLC/MS/MS analysis. TLCA-3-sulfate levels were increased in male *Slc10a1*$^{-/-}$ mice ($p = 0.068$; Fig. 6*C*). We also observed slightly increased TLCA-3-sulfate levels in the sera of female *Slc10a1*$^{-/-}$ mice compared with that of WT mice ($p = 0.321$; Fig. S7*B*). LCA-3-sulfate was not detected in either WT or *Slc10a1*$^{-/-}$ mice. To exclude the possibility that the observed increased TLCA-3-sulfate levels in the serum could have been caused by altered hepatic uptake of this sulfate, we also examined the TLCA-3-sulfate levels in the liver. Compared with WT mice, the liver TLCA-3-sulfate levels increased in both male and female *Slc10a1*$^{-/-}$ mice, which further confirmed the increased BA sulfation under conditions of *Slc10a1* deficiency (Fig. 6*D* and Fig. S7*C*). BA sulfates are more water-soluble and therefore are more readily excreted in urine (13). Indeed, the urinary excretion of TLCA-3-sulfate was significantly increased in *Slc10a1*$^{-/-}$ mice ($p = 0.004$; Fig. 6*E*).

Elevated BA sulfates in human plasma and urine of homozygous p.Ser267Phe mutation in SLC10A1

Based on the findings in mice, we asked whether the BA sulfates also increased in human individuals with p.Ser267Phe mutation in *SLC10A1*. Comprehensive plasma BA profiling of 58 BA species in these individuals was conducted by UPLC/MRM-MS. The concentrations of main primary BAs, including CA, CDCA, and their taurine or glycine conjugates, significantly increased compared with those of healthy controls (Table 2), suggesting hypercholanemia in those p.Ser267Phe variants. For the secondary BAs, DCA and LCA, and their taurine or glycine conjugates, no significant differences were observed (Table 2). We thus could confirm elevated BA sulfates in plasma of homozygous p.Ser267Phe individuals. In particular, the most predominant BA sulfates in the plasma of healthy controls GUDCA-3-sulfate and GLCA-3-sulfate increased from 131.02 ± 132.24 and 130.94 ± 261.36 nM to 1679.92 ± 3229.69 and 400.84 ± 1479.65 nM in p.Ser267Phe variants, respectively (Table 3). Interestingly, some representative atypical BAs detected in these variants were also changed significantly, such as 7-keto-DCA, 7-keto-LCA, Glycine-conjugated

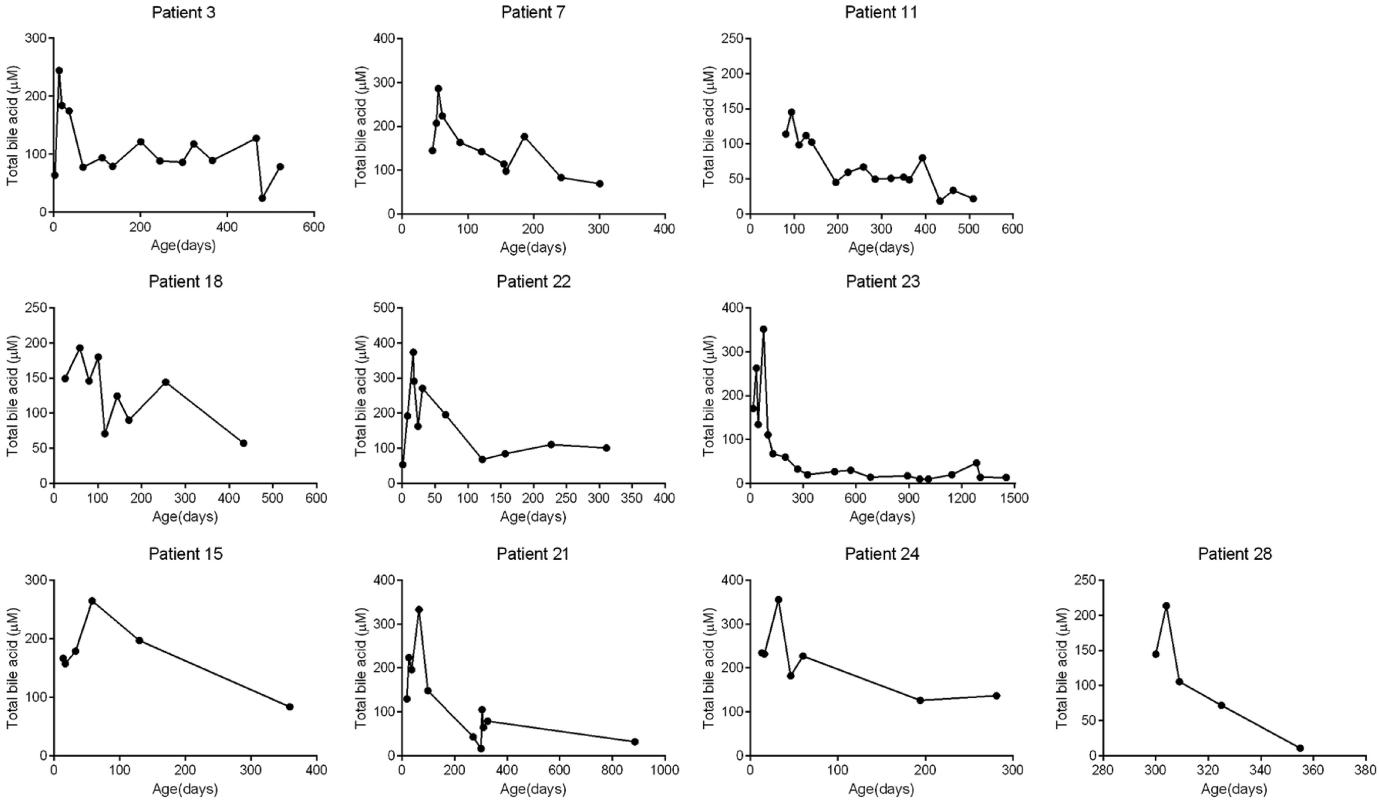

Figure 3. Dynamic analysis of blood bile acid levels in human subjects with p.Ser267Phe variants. Retrospective analysis of blood TBA levels in male (patient IDs: 3, 7, 11, 18, 22, and 23) and female (patient IDs: 15, 21, 24, and 28) p.Ser267Phe variants during their medical processes. Patient ID is indicated *above* each *panel*.

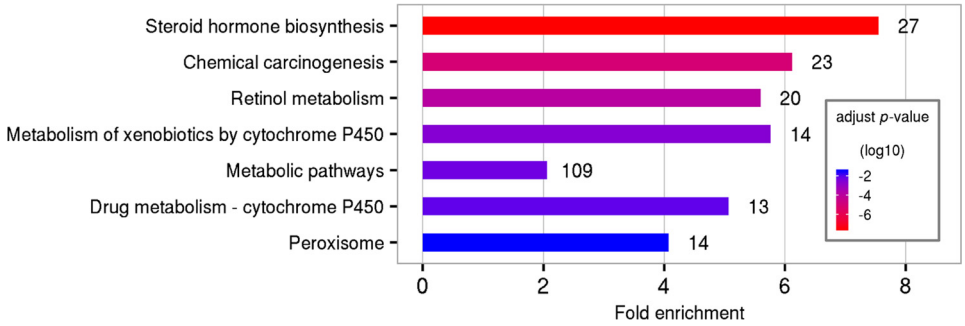

Figure 4. KEGG pathway analysis of differentially expressed gene between male *Slc10a1*$^{-/-}$ and WT mice. Pathways are ranked according to *p* value. *Numbers* on *right* of each pathway indicate the number of differentially expressed genes. Mice were 4 weeks of age ($n = 3$).

hyodeoxycholic acid (GHDCA), TUDCA, nor-UDCA, TβMCA, TλMCA, GλMCA, etc. (Table S2). The p.Ser267Phe individuals also showed a modestly increased ratio of BA sulfates/TBA in urine (Fig. S8), indicating the enhanced urinary clearance of BA sulfates in those individuals with the p.Ser267Phe mutation.

Discussion

We found in this study apparent renormalization of TBA levels over time in mice and humans with *Slc10a1*/*SLC10A1* deficiency, and we report that the renormalization of TBA level is accompanied with increased BA sulfation, suggesting that BA sulfation may underlie the detoxification and elimination of overload BAs both in mice and humans with *Slc10a1*/*SLC10A1* deficiency.

Both in mice and in humans, *Slc10a1*/*SLC10A1* deficiency–related hypercholanemia tends to attenuate as age increases. Indeed, we show that the overall serum TBA levels decrease with age in *Slc10a1*$^{-/-}$ mice, especially in the males, whereas in female *Slc10a1*$^{-/-}$ mice, ~50% persist with moderate hypercholanemia. Nonetheless, the overall survival rate of those hypercholanemic *Slc10a1*$^{-/-}$ mice was not affected (data not shown). The body weights of *Slc10a1*$^{-/-}$ mice were inversely correlated with serum TBA levels, consistent with a previous report (8). Interestingly, we noticed a significant catch-up of body weight gain of *Slc10a1*$^{-/-}$ mice starting from 8 weeks of age, in parallel with TBA declining in these mice. In humans, *SLC10A1* with p.Arg252His variation was the first reported case with NTCP deficiency. The affected individual presented with a relatively mild clinical phenotype at about 2 years old

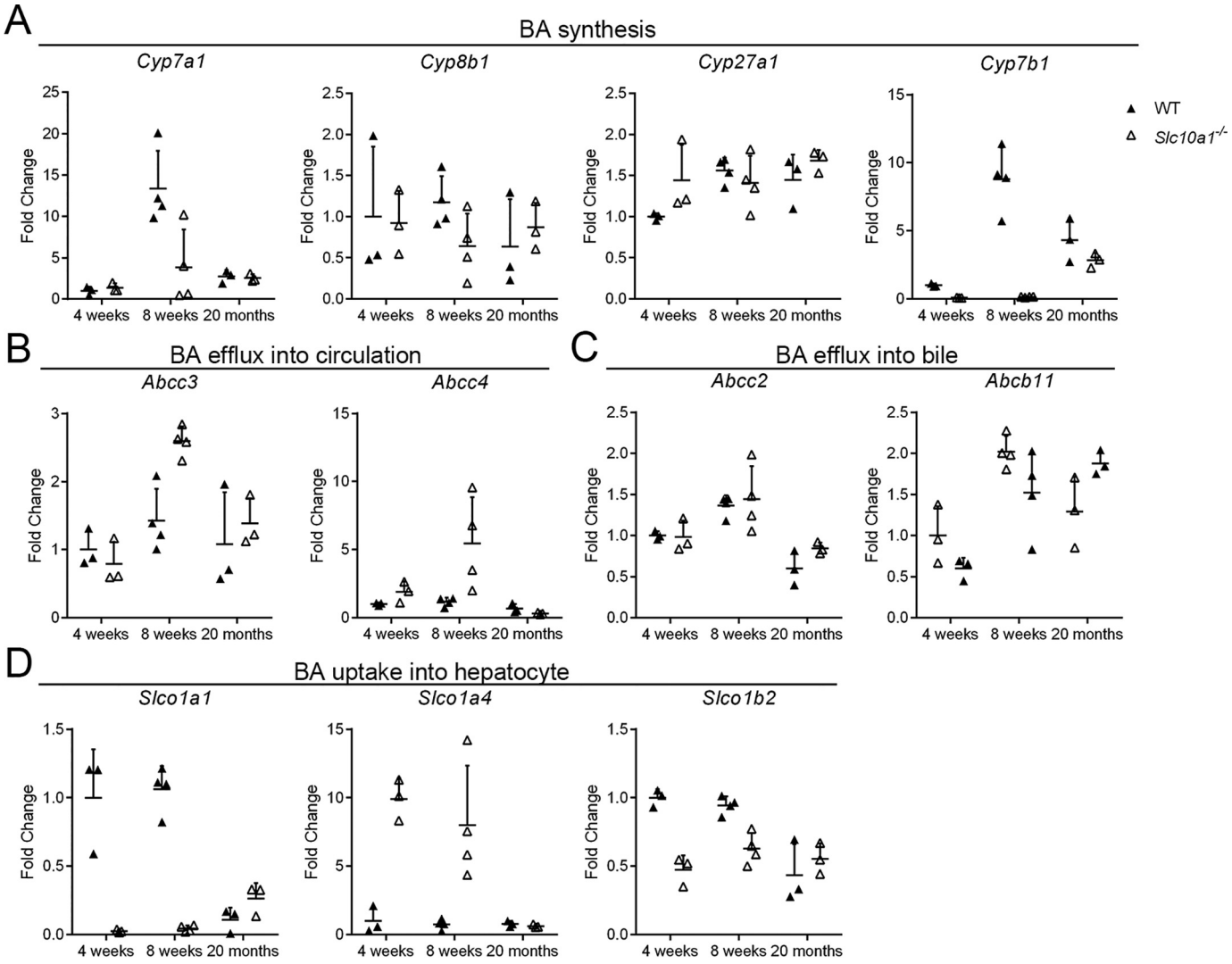

Figure 5. Transcriptional alterations in BA synthesis and transport pathways in male *Slc10a1*$^{-/-}$ mice. Total RNA (n = 3–4) for each time point was prepared, and -fold changes of gene expression with respect to WT at 4 weeks were analyzed using RNA-Seq data. Genes involved in classical and acidic synthesis of BA (*Cyp7a1*, *Cyp8b1*, *Cyp27a1*, and *Cyp7b1*) (*A*), BA efflux into circulation (*Abcc3* and *Abcc4*) (*B*), BA efflux into bile (*Abcc2* and *Abcb11*) (*C*), and BA uptake into hepatocyte (*Slco1a1*, *Slco1a4*, and *Slco1b2*) (*D*) were analyzed. Data are given as mean ± S.D. (*error bars*) of -fold changes to WT at each time point. Data at 8 weeks are a representative result from three independent repeats of RNA-Seq analysis.

Table 1
Top five up-regulated genes in *Slc10a1*$^{-/-}$ mice
Mice were male and 4 weeks of age; TBA > 20 μM. n: read counts normalized by library size.

Gene name	WT mean (n)	*Slc10a1*$^{-/-}$ mean (n)	Fold change ($\log_2$)	Adjusted p
Sult2a1	5	13,069	10.9	6.7E−08
Sult2a2	1	2560	10.1	9.0E−08
Sult1e1	26	14,259	9.0	1.9E−10
Sult2a6	0	432	8.4	4.1E−06
Sult2a4	0	149	7.2	1.6E−03

(TBA up to 1500 μM), and her TBA declined (~500 μM) when she was 8 years old (4, 17). However, in adulthood, humans with NTCP deficiency had a relative mild to normal TBA level (6, 7). In our study, 10 of 33 children with NTCP deficiency exhibited clearly declined TBA levels during the follow-up period; four children still had a TBA level above 100 μM when they were at least 7 years old (data not shown). Long-term follow-up of TBA levels of these individuals is warranted.

A previous study showed that hypercholanemic *Slc10a1*$^{-/-}$ mice displayed changes in expression of hepatic, ileal, and renal BA transporters and enhanced renal BA excretion to attenuate the circulatory BA overload (8). Expression of hepatic *Cyp7a1* was found to be suppressed via induction of ileal *Fgf15* (fibroblast growth factor 15) in the hypercholanemic *Slc10a1*$^{-/-}$ mice (9). In this study, we conducted comprehensive mRNA deep sequencing analysis of *Slc10a1*$^{-/-}$ mice, which provides unbiased information on the metabolism alteration in NTCP-disrupted animals. Remarkably, our results revealed, for the first time, changes of pathways involved in the metabolism of xenobiotics. In particular, the dramatically increased expressions of *Sult* genes implicated enhanced phase II (sulfation) detoxification of BAs in *Slc10a1*$^{-/-}$ mice. Importantly, BA sulfation could be confirmed by UPLC-MS/MS analysis with the presence of TLCA-3-sulfate both in circulation and liver of *Slc10a1*$^{-/-}$ mice. CYP2B10, a phase I hydroxylation enzyme has been indicated to be associated with hydroxylated BAs

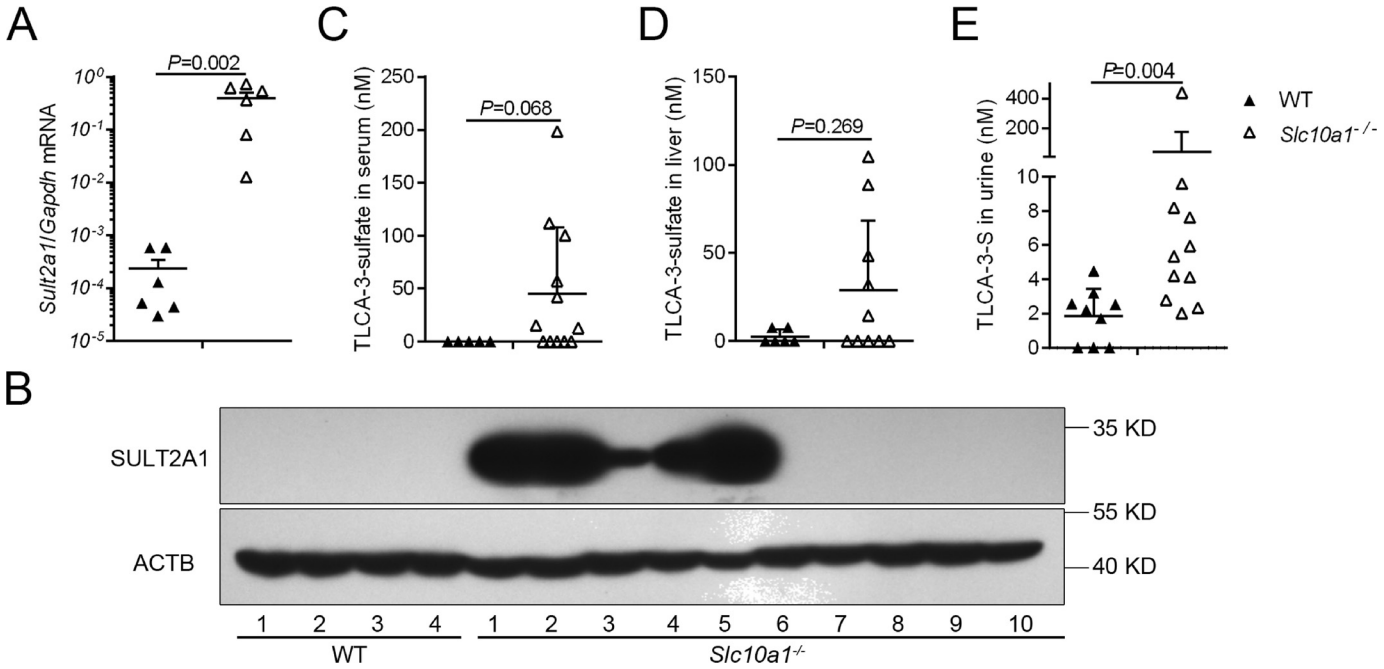

Figure 6. Increased TLCA-3-sulfate in male *Slc10a1*$^{-/-}$ mice. Hepatic SULT2A1 expression was determined by qPCR (*A*) and Western blotting (*B*), respectively. Relative mRNA expression levels were calculated for WT mice and *Slc10a1*$^{-/-}$ mice with high TBA concentrations using the geometric mean of housekeeping gene *Gapdh*. UPLC-MS/MS analysis of TLCA-3-sulfate concentrations in sera (*C*), liver (*D*), and urine (*E*) of *Slc10a1*$^{-/-}$ mice. All male mice are 4 weeks of age. Each *symbol* represents an individual mouse. Two-tailed Mann–Whitney *U* test was used. Values are given as mean ± S.D. (*error bars*) for 5–12 mice/group. In *B*, mice 6–10 expressed CYP2B10 protein (see Fig. S5*D*).

Table 2

Plasma concentrations of main primary and secondary bile acid species in healthy controls and p.Ser267Phe variants

Concentration values are mean ± S.D.

	Healthy controls (n = 43)	p.Ser267Phe (n = 15)	p value, healthy controls/p.Ser267Phe
	nM	nM	
CA	86.9 ± 135.2	819.2 ± 1088.1	0.000
TCA	263.8 ± 614.5	17,434.1 ± 15,473.8	0.000
GCA	1176.7 ± 3165.5	57,694.9 ± 48,102.9	0.000
CDCA	301.2 ± 414.8	615.2 ± 426.1	0.000
TCDCA	687.3 ± 1023.8	7606.3 ± 8174.4	0.000
GCDCA	3581.3 ± 3957.4	67,109.77 ± 44,185.9	0.000
DCA	274.3 ± 491.7	210.4 ± 238.8	0.576
TDCA	43.2 ± 72.1	81.2 ± 193.2	0.776
GDCA	248.1 ± 435.8	1556.5 ± 4825.7	0.852
LCA	3.98 ± 4.07	3.64 ± 6.47	0.093
TLCA	1.21 ± 1.99	0.43 ± 0.58	0.192
GLCA	14.42 ± 27.68	31.94 ± 98.7	0.299

(18–21). Expression of CYP2B10 was also changed significantly in a subtype of *Slc10a1*$^{-/-}$ mice, suggesting the increased BA hydroxylation in *Slc10a1*$^{-/-}$ mice. The enhanced ability of phase I and II detoxification in conditions of NTCP deficiency could be an adaptive response to the overload BAs in the liver (11, 20, 22). Nuclear receptors, such as *Fxr*, *Car*, *Rxr*, and *Pxr* increased and could be responsible for the enhanced BA detoxification (*i.e.* SULT2A1 and CYP2B10) in male *Slc10a1*$^{-/-}$ mice at 4 weeks. However, the molecular mechanism of SULT2A1 and CYP2B10 regulation may be different in *Slc10a1*$^{-/-}$ mice, as those *Slc10a1*$^{-/-}$ mice with high SULT2A1 expression demonstrated a relatively low CYP2B10 expression.

Notably, the increased BA sulfates were also presented in blood and urine of human individuals with the p.Ser267Phe mutation in *SLC10A1*. Therefore, sulfation probably serves as a critical mechanism to decrease BAs' toxic effect and clear the overload BAs both in mice and humans with *Slc10a1*/*SLC10A1* deficiency. Importantly, from the analysis of BA metabolites by UPLC/MRM-MS, we noted that, whereas the concentrations of sulfates of DCA, LCA, and their conjugates were increased in individuals with the p.Ser267Phe variant, the concentrations of DCA, LCA, and their corresponding conjugates were not changed significantly, suggesting that the overall enterohepatic circulation of BAs in those p.Ser267Phe variants was intact. Our study highlighted enhanced BA sulfation in *Slc10a1*/*SLC10A1* deficiency; in such a condition, the BA levels are controlled by coordinated adaptive changes of a phase I bile acid-hydroxylating enzyme, *Cyp2b10*, and a phase II bile acid-sulfating enzyme, *Sult2a1*, in BA metabolism and transportation with transporters of *Abcc3* and *Abcc4* (Fig. 7).

Experimental procedures

Mice studies

Two transcription activator-like effector nuclease (TALEN) constructs targeting 5′-TACGGTATCATGCCCCTCAG-3′ and 5′-TGGTCAGATGAAAGACCTTG-3′ in exon 1 of *Slc10a1* were assembled as described previously (23). C57BL/6 zygotes injected with the TALEN plasmid were transplanted to the ovarian ducts of pseudopregnancy C57BL/6 mice to generate *Slc10a1*$^{-/-}$ mice. A mouse with a 19-bp deletion (5′-TTCTGGGCAAGGTCTTTCA-3′) in exon 1 of *Slc10a1* was chosen as the founder, and all mice used in this study were offspring of the founder mouse. Mice were housed in specific pathogen-free conditions in the animal facility of the National Institute of Biological Sciences (NIBS), Beijing. The current study was approved by the NIBS Institutional Animal Care and Use Committee. Quantitative analysis of serum TBA was conducted

Table 3
Plasma concentrations of some sulfated bile acids species in healthy controls and p.Ser267Phe variants
Concentration values are mean ± S.D.

	Healthy controls (n = 43)	p.Ser267Phe (n = 15)	p value, healthy controls/p.Ser267Phe
	nM	nM	
CA-3–sulfated	1.4 ± 1.89	3.3 ± 2.2	0.000
GCA-3–sulfated	1.82 ± 2.49	9.77 ± 10.31	0.000
DCA-3–sulfated	1.49 ± 2.54	0.95 ± 2.62	0.023
GDCA-3–sulfated	77.99 ± 117.99	166.04 ± 574.13	0.086
TDCA-3–sulfated	12.86 ± 28.58	0.1 ± 0.11	0.233
TCDCA-3–sulfated	98.19 ± 205.54	0.8 ± 1.08	0.136
TLCA-3–sulfated	0.68 ± 1.28	0.06 ± 0.07	0.025
GLCA-3–sulfated	130.94 ± 261.36	400.84 ± 1479.65	0.011
GUDCA-3–sulfated	131.02 ± 132.24	1679.92 ± 3229.69	0.001
TUDCA-3–sulfated	16.2 ± 27.76	0.64 ± 0.74	0.435

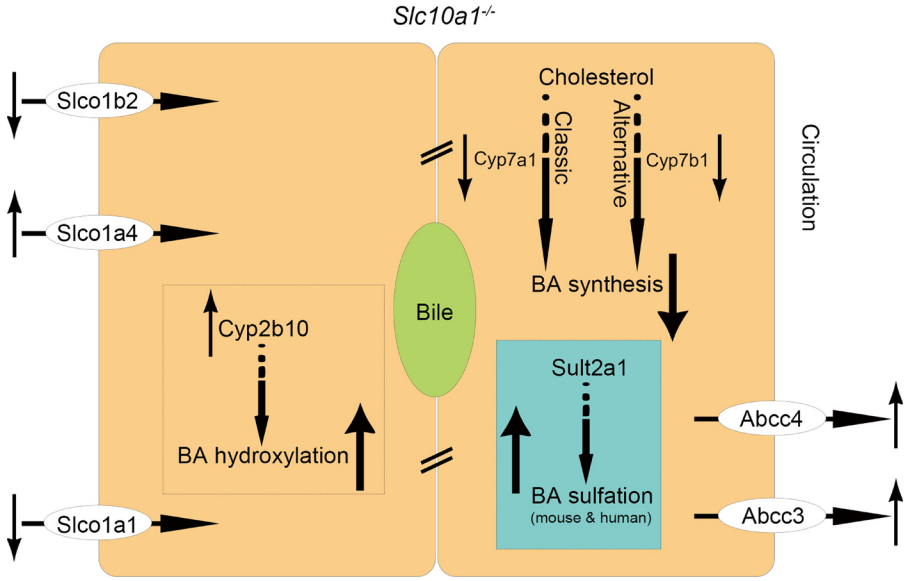

Figure 7. Bile acid sulfation contributes to detoxification of BAs in mice and human with *Ntcp/NTCP* deficiency. In the status of hypercholanemia with *Ntcp* (*Slc10a1*) deficiency, BA synthesis from both the classic (*Cyp7a1*) and alternative (*Cyp7b1*) pathways is decreased. BA sulfation (*Sult2a1*) highlighted in blue box, along with BA hydroxylation (*Cyp2b10*) both are increased to augment the detoxification of overload BAs. Transporters (*Abcc3* and *Abcc4*) effluxing BAs into circulation are up-regulated to facilitate export.

commercially by the Beijing Lawke Health Laboratory Center for Clinical Laboratory Development, Inc. The uptake assay of [^{3}H]taurocholate was described previously (24).

RNA profiling and bioinformatics analysis

Liver mRNA extraction for RNA-Seq and qPCR analysis was described previously (25, 26). Clean mRNA-Seq reads were aligned to the mouse reference genome (GRCm38) with TopHat (version 2.0.13), guided by Ensembl gene annotation v83. Only uniquely aligned and properly paired reads were retained for further analysis. Gene-level read counts were calculated with HTseq (v0.6.1p1) with the union mode. Genes with less than a total of 11 nonnormalized reads across all samples were excluded. Data normalization and statistical analysis of differential expression were performed with the DEseq2 (v1.10.0) R package. Pair-wise Spearman correlation between samples across all quantified genes was used for hierarchical clustering. KEGG pathway enrichment analysis of differentially expressed genes was performed with KOBAS 2.0. Real-time qPCR was performed on CFX96 Touch™ Real-Time PCR Detection System. *Actb* and *Gapdh* were used for internal normalization. Primer sequences used in this study are listed in Table S1.

Biochemical and UPLC/MS/MS analysis

BAs, including αMCA, βMCA, ωMCA, TαMCA, and TβMCA, were purchased from Steraloids. CA, CDCA, DCA, LCA, UDCA, TCA, TCDCA, TDCA, TLCA, TLCA-3-sulfate, TUDCA, GCA, GCDCA, and GUDCA were purchased from Sigma-Aldrich. BAs in serum samples were extracted with the L3 protocol reported by Humbert *et al.* (27). BA extraction from liver samples was conducted using the method described by Alnouti *et al.* (28). For the profiling analysis, the UPLC system was coupled to a Q-Exactive Orbitrap mass spectrometer (Thermo Fisher Scientific) equipped with a heated electrospray ionization (HESI) probe. BA extracts were separated by a BEH C18 100 × 2.1-mm column (Waters). A binary solvent system with mobile phase A containing 100% H_2O, 7.5 mM ammonium acetate (pH 4) and mobile phase B containing MeOH/ACN (95:5) was used over a 25-min gradient with a flow rate of 300 μl/min. Because we were not able to separate the analytical signals for αMCA from ωMCA, their concentrations were calculated together (termed αωMCA); TαMCA and TβMCA are termed TαβMCA. Mouse BA profiling with UPLC-MS/MS was conducted by the National Protein Science Technology Center, Tsin-

ghua University (Beijing, China). MS analysis of TLCA-3-sulfate in urine was conducted by Metabo-Profile (Shanghai, China).

Immunoblotting

Equal amounts of protein from mouse liver were separated by SDS-PAGE and blotted onto polyvinylidene difluoride membranes. The membranes were incubated with primary antibodies overnight at 4 °C. Appropriate peroxidase-conjugated secondary antibodies were applied, and the membranes were visualized by Super Signal Chemiluminescence (Thermo Scientific). The anti-CYP2B10 mAb (sc-53242) and anti-SULT2A1/2/5 mAb (sc-398965) were purchased from Santa Cruz Biotechnology, Inc. Anti-tubulin (BE3312) and anti-ACTB (BE0033) were purchased from EASYBIO.

Human study

This study was approved by Children's Hospital and Jinshan Hospital of Fudan University (Shanghai, China). Each participant provided written informed consent prior to participation in accordance with the ethical guidelines of the 1975 Declaration of Helsinki. Plasma was separated from blood by centrifugation, and urine was collected, aliquoted (50 μl), freeze-dried, and stored at −80 °C until BA profiling. BA analysis was performed by reversed-phase UPLC/MRM-MS with negative ion detection at the UVic-Genome British Columbia Proteomics Centre as described previously (29). The quantitation of BAs utilized standard substances of 58 BAs and 14 deuterium-labeled analogues of BAs as internal standards. These targets, described previously (29, 30), included all of the major BAs.

Statistical analysis

All data are expressed as mean ± S.D. For analysis in mice experiments, inferential statistical significance between two groups was examined using two-tailed Mann–Whitney *U* tests. Two-way ANOVA followed by a Bonferroni post hoc test was used to determine the effect of age or gender interactions. Statistical analyses were conducted using GraphPad Prism version 6.0 (GraphPad Software). For analysis in humans, statistical analysis using the software package IBM SPSS 19.0 was performed to determine differences in the BA profiles between p.Ser267Phe variants and healthy controls. Student's *t* test was performed when the data showed a normal distribution. A nonparametric test, the Mann–Whitney *U* test, was performed when the data did not show a normal distribution. One-way ANOVA followed by a Dunnett's post-hoc test was used to examine the change of TBA levels in infants. p values < 0.05 were considered statistically significant.

Author contributions—F. M., X. H., J.-S. W., and W. L. conceptualization; F. M., T. L., and X. H. data curation; F. M., T. L., X. H., H. Z., and W. L. formal analysis; F. M., X. H., J.-S. W., and W. L. validation; F. M., T. L., X. H., and F. W. investigation; F. M., X. H., and Z. J. visualization; F. M., T. L., X. H., W. H., C. L., X. L., J. H., and C. H. B. methodology; F. M. and X. H. writing-original draft; F. M., T. L., J.-S. W., and W. L. writing-review and editing; H. Z. and Z. J. software; J. S., J. H., and C. H. B. resources; J. S., J. H., C. H. B., J.-S. W., and W. L. funding acquisition; J.-S. W. and W. L. supervision; W. L. project administration.

References

1. Meier, P. J., and Stieger, B. (2002) Bile salt transporters. *Annu. Rev. Physiol.* **64,** 635–661 CrossRef Medline
2. Dawson, P. A., and Karpen, S. J. (2015) Intestinal transport and metabolism of bile acids. *J. Lipid Res.* **56,** 1085–1099 CrossRef Medline
3. Yan, H., Zhong, G., Xu, G., He, W., Jing, Z., Gao, Z., Huang, Y., Qi, Y., Peng, B., Wang, H., Fu, L., Song, M., Chen, P., Gao, W., Ren, B., *et al.* (2012) Sodium taurocholate cotransporting polypeptide is a functional receptor for human hepatitis B and D virus. *eLife* **1,** e00049 CrossRef Medline
4. Vaz, F. M., Paulusma, C. C., Huidekoper, H., de Ru, M., Lim, C., Koster, J., Ho-Mok, K., Bootsma, A. H., Groen, A. K., Schaap, F. G., Oude Elferink, R. P. J., Waterham, H. R., and Wanders, R. J. A. (2015) Sodium taurocholate cotransporting polypeptide (SLC10A1) deficiency: conjugated hypercholanemia without a clear clinical phenotype. *Hepatology* **61,** 260–267 CrossRef Medline
5. Van Herpe, F., Waterham, H. R., Adams, C. J., Mannens, M., Bikker, H., Vaz, F. M., and Cassiman, D. (2017) NTCP deficiency and persistently raised bile salts: an adult case. *J. Inherit. Metab. Dis.* **40,** 313–315 CrossRef Medline
6. Deng, M., Mao, M., Guo, L., Chen, F. P., Wen, W. R., and Song, Y. Z. (2016) Clinical and molecular study of a pediatric patient with sodium taurocholate cotransporting polypeptide deficiency. *Exp. Ther. Med.* **12,** 3294–3300 CrossRef Medline
7. Liu, R., Chen, C., Xia, X., Liao, Q., Wang, Q., Newcombe, P. J., Xu, S., Chen, M., Ding, Y., Li, X., Liao, Z., Li, F., Du, M., Huang, H., Dong, R., *et al.* (2017) Homozygous p.Ser267Phe in SLC10A1 is associated with a new type of hypercholanemia and implications for personalized medicine. *Sci. Rep.* **7,** 9214 CrossRef Medline
8. Slijepcevic, D., Kaufman, C., Wichers, C. G. K., Gilglioni, E. H., Lempp, F. A., Duijst, S., de Waart, D. R., Elferink, R. P., Mier, W., Stieger, B., Beuers, U., Urban, S., and van de Graaf, S. F. J. (2015) Impaired uptake of conjugated bile acids and hepatitis b virus pres1-binding in na(+)-taurocholate cotransporting polypeptide knockout mice. *Hepatology* **62,** 207–219 CrossRef Medline
9. Slijepcevic, D., Roscam Abbing, R. L. P., Katafuchi, T., Blank, A., Donkers, J. M., van Hoppe, S., de Waart, D. R., Tolenaars, D., van der Meer, J. H. M., Wildenberg, M., Beuers, U., Oude Elferink, R. P. J., Schinkel, A. H., and van de Graaf, S. F. J. (2017) Hepatic uptake of conjugated bile acids is mediated by both sodium taurocholate cotransporting polypeptide and organic anion transporting polypeptides and modulated by intestinal sensing of plasma bile acid levels in mice. *Hepatology* **66,** 1631–1643 CrossRef Medline
10. Perez, M. J., and Briz, O. (2009) Bile-acid-induced cell injury and protection. *World J. Gastroenterol.* **15,** 1677–1689 CrossRef Medline
11. Marschall, H. U., Wagner, M., Bodin, K., Zollner, G., Fickert, P., Gumhold, J., Silbert, D., Fuchsbichler, A., Sjövall, J., and Trauner, M. (2006) Fxr(-/-) mice adapt to biliary obstruction by enhanced phase I detoxification and renal elimination of bile acids. *J. Lipid Res.* **47,** 582–592 CrossRef Medline
12. Feng, L., Yuen, Y. L., Xu, J., Liu, X., Chan, M. Y., Wang, K., Fong, W. P., Cheung, W. T., and Lee, S. S. (2017) Identification and characterization of a novel PPARα-regulated and 7α-hydroxyl bile acid-preferring cytosolic sulfotransferase mL-STL (Sult2a8). *J. Lipid Res.* **58,** 1114–1131 CrossRef Medline
13. Alnouti, Y. (2009) Bile acid sulfation: a pathway of bile acid elimination and detoxification. *Toxicol. Sci.* **108,** 225–246 CrossRef Medline
14. Runge-Morris, M., Kocarek, T. A., and Falany, C. N. (2013) Regulation of the cytosolic sulfotransferases by nuclear receptors. *Drug Metab. Rev.* **45,** 15–33 CrossRef Medline
15. Palmer, R. H. (1967) The formation of bile acid sulfates: a new pathway of bile acid metabolism in humans. *Proc. Natl. Acad. Sci. U.S.A.* **58,** 1047–1050 CrossRef Medline
16. Radominska, A., Comer, K. A., Zimniak, P., Falany, J., Iscan, M., and Falany, C. N. (1990) Human liver steroid sulphotransferase sulphates bile acids. *Biochem. J.* **272,** 597–604 CrossRef Medline
17. Vaz, F. M., Huidekoper, H. H., and Paulusma, C. C. (2017) Extended abstract: deficiency of sodium taurocholate cotransporting polypeptide

(SLC10A1): a new inborn error of metabolism with an attenuated phenotype. *Dig. Dis.* **35,** 259–260 CrossRef Medline

18. Wagner, M., Halilbasic, E., Marschall, H.-U., Zollner, G., Fickert, P., Langner, C., Zatloukal, K., Denk, H., and Trauner, M. (2005) CAR and PXR agonists stimulate hepatic bile acid and bilirubin detoxification and elimination pathways in mice. *Hepatology* **42,** 420–430 CrossRef Medline
19. Zollner, G., Wagner, M., Moustafa, T., Fickert, P., Silbert, D., Gumhold, J., Fuchsbichler, A., Halilbasic, E., Denk, H., Marschall, H.-U., and Trauner, M. (2006) Coordinated induction of bile acid detoxification and alternative elimination in mice: role of FXR-regulated organic solute transporter-α/β in the adaptive response to bile acids. *Am. J. Physiol. Gastrointest. Liver Physiol.* **290,** G923–G932 CrossRef Medline
20. Fuchs, C. D., Paumgartner, G., Wahlström, A., Schwabl, P., Reiberger, T., Leditznig, N., Stojakovic, T., Rohr-Udilova, N., Chiba, P., Marschall, H.-U., and Trauner, M. (2017) Metabolic preconditioning protects BSEP/ABCB11$^{-/-}$ mice against cholestatic liver injury. *J. Hepatol.* **66,** 95–101 CrossRef Medline
21. Kulkarni, S. R., S. C. J. Hagey, L. R., Boyer, J. L. (2016) Sirtuin 1 activation alleviates cholestatic liver injury in a cholic acid–fed mouse model of cholestasis. *Hepatology* **64,** 2151–2164 CrossRef Medline
22. Fickert, P., Wagner, M., Marschall, H. U., Fuchsbichler, A., Zollner, G., Tsybrovskyy, O., Zatloukal, K., Liu, J., Waalkes, M. P., Cover, C., Denk, H., Hofmann, A. F., Jaeschke, H., and Trauner, M. (2006) 24-norUrsodeoxycholic acid is superior to ursodeoxycholic acid in the treatment of sclerosing cholangitis in Mdr2 (Abcb4) knockout mice. *Gastroenterology* **130,** 465–481 CrossRef Medline
23. Sanjana, N. E., Cong, L., Zhou, Y., Cunniff, M. M., Feng, G., and Zhang, F. (2012) A transcription activator-like effector toolbox for genome engineering. *Nat. Protoc.* **7,** 171–192 CrossRef Medline
24. Yan, H., Peng, B., Liu, Y., Xu, G., He, W., Ren, B., Jing, Z., Sui, J., and Li, W. (2014) Viral entry of hepatitis B and D viruses and bile salts transportation share common molecular determinants on sodium taurocholate cotransporting polypeptide. *J. Virol.* **88,** 3273–3284 CrossRef Medline
25. He, W., Ren, B., Mao, F., Jing, Z., Li, Y., Liu, Y., Peng, B., Yan, H., Qi, Y., Sun, Y., Guo, J.-T., Sui, J., Wang, F., and Li, W. (2015) Hepatitis D virus infection of mice expressing human sodium taurocholate co-transporting polypeptide. *PLoS Pathog.* **11,** e1004840 CrossRef Medline
26. He, W., Cao, Z., Mao, F., Ren, B., Li, Y., Li, D., Li, H., Peng, B., Yan, H., Qi, Y., Sun, Y., Wang, F., Sui, J., and Li, W. (2016) Modification of three amino acids in sodium taurocholate cotransporting polypeptide renders mice susceptible to infection with hepatitis D virus *in vivo*. *J. Virol.* **90,** 8866–8874 CrossRef Medline
27. Humbert, L., Maubert, M. A., Wolf, C., Duboc, H., Mahé, M., Farabos, D., Seksik, P., Mallet, J. M., Trugnan, G., Masliah, J., and Rainteau, D. (2012) Bile acid profiling in human biological samples: comparison of extraction procedures and application to normal and cholestatic patients. *J. Chromatogr. B Analyt. Technol. Biomed. Life Sci.* **899,** 135–145 CrossRef Medline
28. Alnouti, Y., Csanaky, I. L., and Klaassen, C. D. (2008) Quantitative-profiling of bile acids and their conjugates in mouse liver, bile, plasma, and urine using LC-MS/MS. *J. Chromatogr. B Analyt. Technol. Biomed. Life Sci.* **873,** 209–217 CrossRef Medline
29. Han, J., Liu, Y., Wang, R., Yang, J., Ling, V., and Borchers, C. H. (2015) Metabolic profiling of bile acids in human and mouse blood by LC-MS/MS in combination with phospholipid-depletion solid-phase extraction. *Anal. Chem.* **87,** 1127–1136 CrossRef Medline
30. Qiu, Y. L., Gong, J. Y., Feng, J. Y., Wang, R. X., Han, J., Liu, T., Lu, Y., Li, L. T., Zhang, M. H., Sheps, J. A., Wang, N. L., Yan, Y. Y., Li, J. Q., Chen, L., Borchers, C. H., *et al.* (2017) Defects in myosin VB are associated with a spectrum of previously undiagnosed low γ-glutamyltransferase cholestasis. *Hepatology* **65,** 1655–1669 CrossRef Medline